ARTICLE

De Novo Pathogenic Variants in *CACNA1E* Cause Developmental and Epileptic Encephalopathy with Contractures, Macrocephaly, and Dyskinesias

Katherine L. Helbig,[1,67] Robert J. Lauerer,[2,67] Jacqueline C. Bahr,[2] Ivana A. Souza,[3] Candace T. Myers,[4] Betül Uysal,[2] Niklas Schwarz,[2] Maria A. Gandini,[3] Sun Huang,[3] Boris Keren,[5] Cyril Mignot,[5] Alexandra Afenjar,[6] Thierry Billette de Villemeur,[7] Delphine Héron,[5] Caroline Nava,[5] Stéphanie Valence,[5] Julien Buratti,[5] Christina R. Fagerberg,[8,9] Kristina P. Soerensen,[8] Maria Kibaek,[8] Erik-Jan Kamsteeg,[10] David A. Koolen,[10] Boudewijn Gunning,[11] H. Jurgen Schelhaas,[12] Michael C. Kruer,[13] Jordana Fox,[13] Somayeh Bakhtiari,[13] Randa Jarrar,[13] Sergio Padilla-Lopez,[13] Kristin Lindstrom,[14] Sheng Chih Jin,[15] Xue Zeng,[15] Kaya Bilguvar,[15] Antigone Papavasileiou,[16] Qinghe Xin,[17] Changlian Zhu,[18,19] Katja Boysen,[20] Filippo Vairo,[21] Brendan C. Lanpher,[21] Eric W. Klee,[21] Jan-Mendelt Tillema,[21] Eric T. Payne,[22] Margot A. Cousin,[21,23] Teresa M. Kruisselbrink,[23,24] Myra J. Wick,[23,24] Joshua Baker,[25] Eric Haan,[26]

(Author list continued on next page)

Developmental and epileptic encephalopathies (DEEs) are severe neurodevelopmental disorders often beginning in infancy or early childhood that are characterized by intractable seizures, abundant epileptiform activity on EEG, and developmental impairment or regression. *CACNA1E* is highly expressed in the central nervous system and encodes the α_1-subunit of the voltage-gated $Ca_V2.3$ channel, which conducts high voltage-activated R-type calcium currents that initiate synaptic transmission. Using next-generation sequencing techniques, we identified *de novo CACNA1E* variants in 30 individuals with DEE, characterized by refractory infantile-onset seizures, severe hypotonia, and profound developmental impairment, often with congenital contractures, macrocephaly, hyperkinetic movement disorders, and early death. Most of the 14, partially recurring, variants cluster within the cytoplasmic ends of all four S6 segments, which form the presumed $Ca_V2.3$ channel activation gate. Functional analysis of several S6 variants revealed consistent gain-of-function effects comprising facilitated voltage-dependent activation and slowed inactivation. Another variant located in the domain II S4-S5 linker results in facilitated activation and increased current density. Five participants achieved seizure freedom on the anti-epileptic drug topiramate, which blocks R-type calcium channels. We establish pathogenic variants in *CACNA1E* as a cause of DEEs and suggest facilitated R-type calcium currents as a disease mechanism for human epilepsy and developmental disorders.

Introduction

Developmental and epileptic encephalopathies (DEEs) are clinically and genetically heterogeneous severe neurodevelopmental disorders. These conditions often start in infancy or early childhood and are characterized by intractable seizures, frequent epileptiform activity on EEG, and developmental slowing or regression.[1] A genetic etiology can be identified in upward of 30% of individuals with DEE, predominantly *de novo* variants in genes encoding neuronal ion channels or proteins involved in synaptic transmission.[2]

Voltage-gated calcium channels mediate the influx of calcium in response to membrane depolarization in excitable cells. In presynaptic nerve terminals, this calcium influx triggers transmitter release for synaptic transmission. Several neurological and cardiac disorders are caused by pathogenic variants in genes encoding α_1-subunits of voltage-gated calcium channels, including *CACNA1A* (MIM: 601011) (familial hemiplegic migraine [MIM: 141500], episodic ataxia [MIM: 108500], and epilepsy [MIM: 617106]),[3–5] *CACNA1C* (MIM: 114205) (Timothy syndrome [MIM: 601005]),[6,7] *CACNA1D* (MIM: 114206) (primary aldosteronism, neurodevelopmental disorders

[1]Division of Neurology, Children's Hospital of Philadelphia, Philadelphia, PA 19104, USA; [2]Department of Neurology and Epileptology, Hertie Institute for Clinical Brain Research, University of Tübingen, 72076 Tübingen, Germany; [3]Department of Physiology & Pharmacology, Hotchkiss Brain Institute and Alberta Children's Hospital Research Institute, University of Calgary, Calgary, AB T2N 1N4, Canada; [4]Division of Genetic Medicine, University of Washington, Seattle, WA 98195, USA; [5]APHP, Département de Génétique, Centre de Référence Déficiences Intellectuelles de Causes Rares, Groupe Hospitalier Pitié Salpêtrière et GHUEP Hôpital Trousseau; Sorbonne Université, GRC "Déficience Intellectuelle et Autisme," 75013 Paris, France; [6]Sorbonne Université, GRC n°19, Pathologies Congénitales du Cervelet-LeucoDystrophies, Département de Génétique et Embryologie Médicale, AP-HP, Hôpital d'Enfants Armand Trousseau, Centre de Référence des Déficits Intellectuels de Causes Rares, 75012 Paris, France; [7]Sorbonne Université, GRC n°19, Pathologies Congénitales du Cervelet-LeucoDystrophies, Service de Neuropédiatrie, AP-HP, Hôpital d'Enfants Armand Trousseau; Centre de Référence des Déficits Intellectuels de Causes Rares; Inserm U 1141, 75012 Paris, France; [8]Department of Clinical Genetics, Odense University Hospital, 5000 Odense, Denmark; [9]H.C. Andersen Children's Hospital, Odense University Hospital, 5000 Odense, Denmark; [10]Department of Human Genetics, Radboud University Medical Center, 6525 Nijmegen, the Netherlands; [11]Stichting Epilepsie Instellingen Nederland, 8025 Zwolle, the Netherlands; [12]Department of Neurology, Academic Center for

(Affiliations continued on next page)

Nicholas Smith,[27] Mark A. Corbett,[28] Alastair H. MacLennan,[28] Jozef Gecz,[28] Saskia Biskup,[29] Eva Goldmann,[30] Lance H. Rodan,[31,32] Elizabeth Kichula,[1] Eric Segal,[33] Kelly E. Jackson,[34] Alexander Asamoah,[34] David Dimmock,[35] Julie McCarrier,[35] Lorenzo D. Botto,[36] Francis Filloux,[37] Tatiana Tvrdik,[38] Gregory D. Cascino,[22] Sherry Klingerman,[22] Catherine Neumann,[39] Raymond Wang,[39,40] Jessie C. Jacobsen,[41] Melinda A. Nolan,[42] Russell G. Snell,[41] Klaus Lehnert,[41] Lynette G. Sadleir,[43] Britt-Marie Anderlid,[44,45] Malin Kvarnung,[45] Renzo Guerrini,[46] Michael J. Friez,[47] Michael J. Lyons,[47] Jennifer Leonhard,[48] Gabriel Kringlen,[49] Kari Casas,[49] Christelle M. El Achkar,[50,51] Lacey A. Smith,[50] Alexander Rotenberg,[51,52] Annapurna Poduri,[50,51] Alba Sanchis-Juan,[53,54] Keren J. Carss,[53,54] Julia Rankin,[55] Adam Zeman,[56] F. Lucy Raymond,[54,57] Moira Blyth,[58] Bronwyn Kerr,[59,60] Karla Ruiz,[61] Jill Urquhart,[60] Imelda Hughes,[61] Siddharth Banka,[59,60] Deciphering Developmental Disorders Study,[62] Ulrike B.S. Hedrich,[2] Ingrid E. Scheffer,[20,63,64,65] Ingo Helbig,[1,66] Gerald W. Zamponi,[3] and Holger Lerche,[2,67] and Heather C. Mefford[4,67,*]

[MIM: 615474]),[8,9] and *CACNA1G* (MIM: 604065) (spinocerebellar ataxia [MIM: 616795]).[10–12] *CACNA1E* (MIM: 601013) is located on chromosome 1q25.3 and encodes the functionally critical α_{1E}-subunit of the Ca_V2 family member $Ca_V2.3$, which is widely expressed throughout the central nervous system and conducts high-voltage-activated, rapidly inactivating R-type calcium currents, which are used to initiate rapid synaptic transmission.[13–15] *CACNA1E* plays a role in rodent models of acquired epilepsy,[16,17] and a recent meta-analysis of whole-exome sequencing data of nearly 7,000 individuals with neurodevelopmental disorders implicates *CACNA1E* as a possible candidate gene.[18] However, in contrast to the other α_1-subunits, pathogenic variants in *CACNA1E* have not been established as disease causing in humans.

Here, we clinically and functionally characterize a disorder of neuronal calcium channel dysfunction, caused by *de novo* missense variants in *CACNA1E*. We report 30 individuals who present with a spectrum of severe early-onset neurodevelopmental disorders characterized by severe to profound global developmental delay, significant hypotonia, and developmental and epileptic encephalopathy.

Epileptology, Kempenhaeghe and Maastricht UMC, 5591 Heeze, the Netherlands; [13]Barrow Neurological Institute, Phoenix Children's Hospital, Departments of Child Health, Genetics, Neurology, and Cellular & Molecular Medicine, University of Arizona College of Medicine, Phoenix, AZ 85013, USA; [14]Division of Genetics and Metabolism, Phoenix Children's Hospital, Phoenix, AZ 85016, USA; [15]Yale School of Medicine, New Haven, CT 06510, USA; [16]Department of Pediatric Neurology, Penteli Children's Hospital, 152 36 Athens, Greece; [17]Institute of Biomedical Science and Children's Hospital Fudan University, 201102 Shanghai, China; [18]Perinatal Center, Sahlgrenska Academy, Gothenburg University, 413 46 Gothenburg, Sweden; [19]Hospital of Zhengzhou University, 450001 Zhengzhou, China; [20]Epilepsy Research Centre, Department of Medicine, The University of Melbourne, Austin Health, Heidelberg, VIC 3084, Australia; [21]Department of Health Science Research, Mayo Clinic, Rochester, MN 55905, USA; [22]Department of Neurology, Mayo Clinic College of Medicine, Rochester, MN 55905, USA; [23]Center for Individualized Medicine, Mayo Clinic, Rochester, MN 55905, USA; [24]Department of Clinical Genomics, Mayo Clinic, Rochester, MN 55905, USA; [25]University of Illinois Chicago College of Medicine, University of Illinois College of Medicine at Peoria, Peoria, IL 61605, USA; [26]Adult Genetics Unit, Royal Adelaide Hospital, and School of Medicine, University of Adelaide, Adelaide, SA 5000, Australia; [27]Department of Neurology, Women's and Children's Hospital, University of Adelaide, North Adelaide, SA 5006, Australia; [28]Adelaide Medical School, Robinson Research Institute, University of Adelaide, North Adelaide, SA 5006, Australia; [29]CeGaT, 72076 Tübingen, Germany; [30]Department of Human Genetics, University of Tübingen, 72076 Tübingen, Germany; [31]Division of Genetics and Genomics and Department of Neurology, Boston Children's Hospital, Boston, MA 02115, USA; [32]Department of Pediatrics, Harvard Medical School, Boston, MA 02215, USA; [33]Northeast Regional Epilepsy Group, Hackensack University Medical Center, Hackensack, NJ 07601, USA; [34]University of Louisville, Louisville, KY 40292, USA; [35]Children's Hospital of Wisconsin, Milwaukee, WI 53226, USA; [36]Division of Medical Genetics, Department of Pediatrics, University of Utah, Salt Lake City, UT 84113, USA; [37]Division of Pediatric Neurology, Departments of Pediatrics and Neurology, University of Utah, Salt Lake City, UT 84113, USA; [38]ARUP Laboratories, Salt Lake City, UT 84108, USA; [39]Division of Metabolic Disorders CHOC Children's Hospital, Orange, CA 92868, USA; [40]Department of Pediatrics, University of California-Irvine School of Medicine, Irvine, CA 92617, USA; [41]Centre for Brain Research and School of Biological Sciences, The University of Auckland, Auckland 1142, New Zealand; [42]Department of Neurology, Starship Children's Health, Auckland 1023, New Zealand; [43]Department of Paediatrics and Child Health, University of Otago Wellington, Wellington South 6242, New Zealand; [44]Department of Clinical Genetics, Karolinska University Hospital, 171 76 Stockholm, Sweden; [45]Department of Molecular Medicine and Surgery, Karolinska Institutet, 171 77 Stockholm, Sweden; [46]Department of Neuroscience, Azienda Ospedaliero-Universitaria Meyer, University of Florence, 50139 Florence, Italy; [47]Greenwood Genetic Center, Greenwood, SC 29646, USA; [48]Medical Genetics, Sanford Health, Bemidji, MN 56601, USA; [49]Medical Genetics, Sanford Health, Fargo, ND 58102, USA; [50]Epilepsy Genetics Program, Department of Neurology, Boston Children's Hospital, Boston, MA 02115, USA; [51]Department of Neurology, Harvard Medical School, Boston, MA 02215, USA; [52]Department of Neurology, Boston Children's Hospital, Boston, MA 02115, USA; [53]Department of Haematology, University of Cambridge, NHS Blood and Transplant Centre, Cambridge CB2 0QQ, UK; [54]NIHR BioResource - Rare Diseases, Cambridge University Hospitals NHS Foundation Trust, Cambridge Biomedical Campus, Cambridge CB2 0QQ, UK; [55]Clinical Genetics, Royal Devon and Exeter NHS Foundation Trust, Exeter EX2 5DW, UK; [56]Department of Neurology, Royal Devon and Exeter NHS Foundation Trust, Exeter EX2 5DW, UK; [57]Department of Medical Genetics, Cambridge Institute for Medical Research, University of Cambridge, Cambridge CB2 0XY, UK; [58]Yorkshire Regional Genetics Service, Chapel Allerton Hospital Leeds Teaching Hospitals NHS Trust, Leeds LS7 4SA, UK; [59]Division of Evolution and Genomic Sciences, School of Biological Sciences, Faculty of Biology, Medicine and Health, The University of Manchester, Manchester M13 9PL, UK; [60]Manchester Centre for Genomic Medicine, St. Mary's Hospital, Manchester University Foundation NHS Trust, Health Innovation, Manchester M13 9WL, UK; [61]Department of Paediatric Neurology, Royal Manchester Children's Hospital, Manchester University Foundation NHS Trust, Health Innovation, Manchester M13 9WL, UK; [62]Wellcome Sanger Institute, Cambridge CB10 1SA, UK; [63]The Florey Institute and Murdoch Children's Research Institute, Parkville, VIC 3052, Australia; [64]Department of Paediatrics, The University of Melbourne, Royal Children's Hospital, Parkville, VIC 3052, Australia; [65]Department of Neurology, Royal Children's Hospital, Parkville, VIC 3052, Australia; [66]Department of Neuropediatrics, Christian-Albrechts-University of Kiel, 24105 Kiel, Germany
[67]These authors contributed equally to this work
*Correspondence: hmefford@uw.edu
https://doi.org/10.1016/j.ajhg.2018.09.006.

Subjects and Methods

Study Participants

This study was approved by the local institutional review boards of the participating centers. Informed consent for participation in this study was provided by all parents or legal guardians of minors or individuals with intellectual disability. Individuals with likely pathogenic *CACNA1E* variants were ascertained between June 2015 and May 2018 via an international collaborative network of research and diagnostic sequencing laboratories. Some participants were identified via GeneMatcher.[19] Individual 16 was ascertained from the Epi4K study.[20] Individuals 23 and 26 were ascertained from the Deciphering Developmental Disorders Study.[21] Individual 31 was ascertained from the UK National Institute for Health Research (NIHR) Bioresource for Rare Diseases.[22] The remaining participants were referred from collaborating researchers, clinicians, and diagnostic laboratories. Detailed medical history information, including developmental and epilepsy history, morphologic details, and neurological findings, was provided for each participant. Where required, reverse phenotyping was performed.[23] Available brain imaging and EEG data were reviewed for all participants. Epilepsy syndromes and seizure types were classified according to the International League Against Epilepsy (ILAE) classification criteria.[24,25]

Variant Identification and Interpretation

Whole-Exome Sequencing

Trio whole-exome sequencing (WES) was performed on a diagnostic basis at GeneDx for individuals 1, 5, 6, 11, and 25 as previously described,[26] at Ambry Genetics for individuals 13, 14, 20, and 29,[27] and at ARUP Laboratories for individual 15 (Supplemental Subjects and Methods). Research-based trio WES was performed for individuals 3, 4, 7–9, 16–19, 21–23, 26–28, and 33. Individual 30 underwent WES as a mother-proband duo. Trio WES was performed as described previously for individual 16 as part of the Epi4K project.[20] Individuals 23 and 26 were ascertained by reanalysis of the data from the Deciphering Developmental Disorders Study[28] as part of a local "Solving the Unsolved" project in Manchester (UK) and a Complementary Analysis Project #237.[21] Trio WES was performed for individual 27 as described previously.[29] Sequencing methodology for the remaining participants is detailed in the Supplemental Subjects and Methods. All candidate variants identified via WES were validated by Sanger sequencing, except for the recurrent c.1054G>A (p.Gly352Arg) variant in individual 8.

Whole-Genome Sequencing

Research-based trio whole-genome sequencing (WGS) was performed in individuals 10, 24, and 31, as described in the Supplemental Subjects and Methods. Candidate variants identified via WGS were validated by Sanger sequencing.

NGS Panel Analysis

Individual 12 underwent diagnostic NGS-based 1430 gene epilepsy panel testing (GeneDx). Individuals 2 and 32 underwent research epilepsy panel testing, as previously described.[30] The presence or absence of variants identified via epilepsy panel testing was confirmed via Sanger sequencing in participants and parents. Parental relationships were confirmed for individuals 2 and 12 by short tandem repeat analysis. Parental DNA samples were unavailable for individual 32.

Variant Interpretation

All identified *CACNA1E* variants were interpreted according to the American College of Medical Genetics and Genomics standards and guidelines for the interpretation of sequence variants.[31] *CACNA1E* variants were considered likely pathogenic if they were confirmed to have occurred *de novo* in the affected individual with confirmed parental relationships and were not observed in a control cohort of 123,136 individuals in the Exome Aggregation Consortium (ExAC)[32] or genome Aggregation Database (gnomAD).

Functional Analysis

Two laboratories independently investigated the effects of the domain II S6 and the domain II S4-S5 linker variants. Given the congruence of findings from these two groups, we combined the results into a single study. The two laboratories used different $Ca_V2.3$ channel backbones for mutagenesis and slightly different experimental setups and approaches. In each case, appropriate wild-type controls were used, and no direct statistical comparisons between the two datasets were made. Prior studies characterizing the structure and function of $Ca_V2.3$ channels had examined the biophysical and electrophysiological properties of several variants that were artificially introduced into S6 segments of $Ca_V2.3$ channels, including p.Arg352Gly, p.Ile701Val/Gly, and p.Ala1720Gly.[33,34] These prior findings were also compared with the results of our functional analyses.

Mutagenesis

The human $Ca_V2.3$-subunit ($\alpha_{1E\text{-}1}$; GenBank: NM_001205293.1) in the pcDNA3.1 vector was kindly provided by Norbert Klugbauer (Institute for Experimental and Clinical Pharmacology and Toxicology, Albert-Ludwigs-Universität Freiburg, Freiburg, Germany),[35] whereas human $Ca_V2.3$ ($\alpha_{1E\text{-}3}$, GenBank: L29385.1) was provided by Dr. Toni Schneider (University of Cologne). The human β_{2d}-subunit cloned into a pIRES2-EGFP-Vector (Clontech) was from Stefan Herzig (Department of Pharmacology, University of Cologne, Cologne, Germany). Site-directed mutagenesis was performed to engineer the domain II S6 segment variants into the human $Ca_V2.3$ channel ($\alpha_{1E\text{-}1}$) using the Q5-Site directed mutagenesis kit (New England Biolabs; primers are available upon request). To exclude incorrect ligation of the plasmid, a diagnostic restriction digest was performed. The p.Ile603Leu domain II S4-S5 linker variant was introduced into $Ca_V2.3$ ($\alpha_{1E\text{-}3}$) channel in pcDNA3 using the QuikChange II XL Site-Directed Mutagenesis Kit (Agilent, Cat# 200521). In each case, the mutant cDNA was then fully re-sequenced before use in experiments to confirm the introduced variant and exclude any additional sequence alterations.

Transfection and Expression in tsA201 Cells

Human tsA201 cells, a transformed human kidney cell line stably expressing an SV40 temperature-sensitive T antigen (Sigma-Aldrich), were cultured at 37°C, with 5% CO_2 humidified atmosphere and grown in Dulbecco's modified Eagle medium + 10% (v/v) fetal bovine serum. For the domain II S6 mutants, transfections using "TransIT-LT1" reagent (Mirus Bio) were performed for transient expression of wild-type or mutant α-subunits together with the β_{2d}-subunit. We transfected 3.16 μg of total DNA in a molar ratio of 1:1. Only cells with green fluorescence were used for electrophysiological recordings. For the domain II S6 variants, we performed electrophysiological recordings of tsA201 cells that were transiently transfected with either wild-type or mutant α_{1E}-subunits together with the β_{2d}-subunit, confirmed by the green fluorescence of EGFP which was co-expressed via an internal ribosome entry site (IRES). For the domain II S4-S5 mutant and corresponding wild-type control, cells were transfected with $Ca_V2.3$

and rat β_{1b} and $\alpha_2\delta$ subunits (3 μg each) along with eGFP, using the calcium phosphate method.

Electrophysiology

Standard whole-cell recordings were performed using an Axopatch 200B amplifier, a Digidata 1320A or Digidata 1440A digitizer, and pCLAMP 8 or 10.2 data acquisition software (Molecular Devices). Leakage and capacitive currents were automatically subtracted using a pre-pulse protocol (-P/4) for the domain II S6 variants. Currents were filtered at 3 or 5 kHz and digitized at 10 kHz. All recordings were performed at room temperature of 21°C–23°C. The liquid junction potential was calculated to be at 10.3 mV using pCLAMP 10.4 software and was not corrected. Cells were visualized using an inverted microscope (Axio-Vert.A1, Zeiss or DM IL LED, Leica or Nikon TE200). For investigation of the domain II S6 variants, the pipette solution contained (in mM): 105 CsF, 30 CsCl, 10 EGTA, 1 $MgCl_2$, 10 (4-(2-hydroxyethyl)-1-piperazineethanesulphonic acid (HEPES) (pH 7.4; 310 mOsm). The bath solution contained (in mM) 15 $BaCl_2$, 150 Choline-Cl, 1 $MgCl_2$, 10 HEPES (pH 7.4; 320 mOsm). For both solutions pH was adjusted with CsOH and osmolarity with Mannitol if necessary. Ba^{2+} currents of 0.4–4 nA were recorded from transfected tsA201 cells.

For the domain II S4-S5 variant and wild-type controls, external solutions contained in (mM): 2 $CaCl_2$, 137 CsCl, 1 $MgCl_2$, 10 HEPES, 10 glucose (pH 7.4 adjusted with CsOH) or 5 mM $BaCl_2$, 132.5 CsCl, 1 $MgCl_2$, 10 HEPES, 10 glucose (pH 7.4, adjusted with CsOH). The pipette solution contained (in mM): 130 CsCl, 2.5 $MgCl_2$, 10 HEPES, 10 EGTA, 3 ATP, 0.5 GTP (pH 7.4 adjusted with CsOH). Borosilicate glass pipettes had a final tip resistance of 1–2 MΩ when filled with internal recording solution. We carefully checked that the maximal voltage error due to residual series resistance after up to 95% compensation was always <5 mV.

Voltage Clamp Protocols and Data Analysis

The membrane was depolarized to various test potentials from a holding potential of −90 mV to record Ba^{2+} currents. The activation curve (conductance-voltage relationship) was derived from the current-voltage relationship obtained by plotting the peak current against various step depolarizations according to:

$$g(V) = \frac{I}{V - V_{rev}}$$

with g being the conductance, I the recorded peak current at test potential V, and V_{rev} the apparent observed Ba^{2+} reversal potential. Although the I-V relationship was not free of gating disturbances, we determined the apparent reversal potential by fitting the current-voltage relationship between −70 mV and 20 mV.

The following Boltzmann function was fit to the conductance-voltage relationship:

$$g(V) = \frac{g_{max}}{1 + e^{\left(-\frac{V - V_{1/2}}{k_V}\right)}}$$

with g being the conductance at test potential V, g_{max} the maximal conductance, $V_{1/2}$ the voltage of half-maximal activation, and k_V a slope factor.

The residual current r400 was determined by dividing the peak Ba^{2+} current I_{Peak} of each current trace by the mean residual current I_{res} during the last 10 ms of a 400 ms voltage pulse. Channels were not completely inactivated at this time point, so that this value served as a surrogate parameter of the time course of inactivation. For wild-type and domain II S4-S5 mutant channels coexpressed with β_{1b}, inactivation kinetics were quantified using monoexponential fits. To assess the time course of activation, a first-order exponential function was fitted to the current trace using ClampFit, yielding the activation time constant τ_{act}.

Data and Statistical Analysis

For variants in the domain II S6 segment, traces were displayed offline with pClamp 10.4 (Molecular Devices). Fits were performed using gnuplot 5.0 (Freeware, T. Williams & C. Kelley). Graphics were generated using a combination of Microsoft Excel (Microsoft Corporation) and Origin (version 2018; OriginLab) software, and statistics were performed using SigmaPlot 12.0 (Statcon). We recorded r400 values at different potentials but performed statistical testing only for a single potential i.e., 5 mV. For the voltage dependence of r400 and also for τ_{act}, we calculated the area under the curve as trapezoids using all data points between −17.5 mV and 42.5 mV. The resulting sum was used for statistical testing. All data were tested for normal distribution. For statistical evaluation, ANOVA on ranks (Kruskal-Wallis-Test) with Dunn's posthoc test for not normally distributed data or one-way ANOVA (Bonferroni posthoc test) was used when datasets were normally distributed. All data are shown as means ± SEM. Boxes in boxplots indicate the interquartile range. Whiskers show the 5^{th} and 95^{th} percentiles.

For the domain II S4-S5 linker p.Ile603Leu variant, data were analyzed using the Clampfit 10.3 software (Molecular Devices) and fit using GraphPad Prism 6. Averaged data are plotted as mean ± SEM and statistical analysis was performed using Student's t test or ANOVA, where $p \leq 0.05$ was considered significant.

Results

Clinical Characteristics

We identified 30 unrelated individuals with missense variants in *CACNA1E* (GenBank: NM_000721.3). A picture of a profound DEE emerged, with affected individuals typically having pharmaco-resistant seizures beginning in the first year of life, profound developmental impairment, hyperkinetic movement disorders, and severe axial hypotonia (Tables 1 and S1). Of the probands older than 2 years, 21/24 (88%) were non-verbal and non-ambulatory. Developmental regression occurred in 9/30 (30%) individuals, often in association with seizure onset. All affected individuals had prominent axial hypotonia, often with appendicular hypertonia; spastic quadriplegia was reported in 16/30 (53%) individuals. 13/30 (43%) affected individuals had congenital joint contractures ranging from isolated talipes equinovarus to arthrogryposis multiplex congenita, frequently prompting initial consideration of a congenital neuromuscular disorder.

Epilepsy was present in 26/30 (87%) individuals, with median age of seizure onset of 4.5 months (range 1 day to 47 months). Seizures began in the first year of life in 21/25 (84%) individuals for whom data were available. Epileptic spasms were the most common initial seizure type (14/26; 54%) followed by focal motor seizures (5/26; 19%). Most individuals (20/26; 77%) developed additional seizure types (Table S1); status epilepticus occurred in two individuals. Four individuals had no seizures identified (at age 1–4 years).

Table 1. Phenotypic and Genetic Features of Individuals with Disease-Causing *CACNA1E* Missense Variants

	Age (Sex)	Variant (NM_000721.3)	Seizure Types (Age of Onset of First Seizure)	EEG	MRI	Neurological Features	Development	Movement Disorder	Congenital Contractures	Macrocephaly
Individual 1	3y (M)	c.683T>C (p.Leu228Pro) *de novo*	Myo (2w), FIAS	multifocal discharges	white matter volume loss	spastic quadriplegia, hypotonia	profound DD: NV, NA	–	–	–
Individual 2	2y (F)	c.1042G>C (p.Gly348Arg) *de novo*	ES (7 m), FIAS, GTCS, Myo	hyps, multifocal discharges	normal	severe truncal hypotonia, appendicular hypertonia	profound DD: NV, NA	dystonia	–	–
Individual 3	25y (F)[a]	c.1054G>A (p.Gly352Arg) *de novo*	T (3y), FIAS, GTCS, Myo, gel	multifocal discharges	normal	spastic quadriplegia, hypotonia	profound DD: NV, NA	dystonia	+	+
Individual 4	5.5y (F)	c.1054G>A (p.Gly352Arg) *de novo*	T (3y), GTCS	multifocal discharges	normal	spastic dystonic quadriplegia, hypotonia	profound DD: NV, NA	dystonia	–	+
Individual 5	16y (M)	c.1054G>A (p.Gly352Arg) *de novo*	ES (10 m), GTCS	slow spike-wave	normal	hypotonia, appendicular hypertonia	profound DD: NV, NA	dystonia	–	+
Individual 6	2y (M)[a]	c.1054G>A (p.Gly352Arg) *de novo*	FM (2 m), ES	multifocal discharges	cortical atrophy	severe axial hypotonia, appendicular hypertonia	profound DD: NV, NA	dystonia	–	–
Individual 7	8y (F)	c.1054G>A (p.Gly352Arg) *de novo*	ES (4 m)	multifocal discharges	cortical atrophy	spastic dystonic quadriplegia	profound DD: NV, NA	dystonia	–	–
Individual 8	6y (F)	c.1054G>A (p.Gly352Arg) *de novo*	FM (14 m), T (14 m)	multifocal discharges; CSWS	white matter volume loss	hypotonia	profound DD: NV, NA	dystonia	+	–
Individual 9	12y (F)	c.1054G>A (p.Gly352Arg) *de novo*	FM (6 m), FIAS, T	temporal spikes	hyperintense T2 signal in parieto-occipital region	severe axial hypotonia, neck dystonia	profound DD: NV, NA	dystonia, chorea	+	+
Individual 10	15y (M)	c.1054G>A (p.Gly352Arg) *de novo*	ES (4 m), GTCS, T, FIAS	hyps, polyspike-wave	normal	severe axial hypotonia, appendicular hypertonia	profound DD: NV, NA	dystonia, dyskinesia, myoclonus	+	–
Individual 11	1y (F)	c.1054G>A (p.Gly352Arg) *de novo*	-	multifocal discharges	normal	severe axial hypotonia, appendicular hypertonia	profound DD: NV	dystonia	+	+
Individual 12	1.5y (M)	c.1807A>C (p.Ile603Leu) *de novo*	FM (7 m)	multifocal discharges	normal	severe hypotonia, hyporeflexia	profound DD: NV, NA	–	–	–
Individual 13	2y (F)	c.2069G>A (p.Gly690Asp) *de novo*	-	multifocal discharges	normal	severe diffuse hypotonia	profound DD: NV, NA	dystonia, hyperkinetic	–	–

(*Continued on next page*)

Table 1. ***Continued***

	Age (Sex)	Variant (NM_000721.3)	Seizure Types (Age of Onset of First Seizure)	EEG	MRI	Neurological Features	Development	Movement Disorder	Congenital Contractures	Macrocephaly
Individual 14	4y (F)[a]	c.2093T>C (p.Phe698Ser) *de novo*	ES (1w), T	hyps, multifocal discharges	normal	profound hypotonia	profound DD: NV, NA	–	+	–
Individual 15	8y (F)	c.2098G>A (p.Ala700Thr) *de novo*	Myo (19 m), GTCS	hyps, multifocal discharges	normal	severe diffuse hypotonia	profound DD: NV, NA	–	–	–
Individual 16	9y (F)	c.2101A>G (p.Ile701Val) *de novo*	ES (9 m), FIAS	multifocal discharges	normal	hypotonia, appendicular hypertonia	profound DD: NV, NA	dystonia, chorea	–	–
Individual 17	18y (F)	c.2101A>G (p.Ile701Val) *de novo*	T (5 m), FM	multifocal discharges	cortical atrophy	hypotonia	profound DD: NV, NA	–	–	+
Individual 18	10y (F)	c.2101A>G (p.Ile701Val) *de novo*	ES (9 m), FIAS	multifocal discharges	normal	severe axial hypotonia, appendicular hypertonia	profound DD: NV, NA	chorea	–	+
Individual 19	1.5y (M)	c.2104G>A (p.Ala702Thr) *de novo*	ES (4 m), FM, Myo, T	multifocal discharges, hyps	Normal	severe axial hypotonia, appendicular hypertonia	profound DD: NV	–	–	+
Individual 20	1y (M)	c.2104G>A (p.Ala702Thr) *de novo*	ES (4 m), T	hyps	normal	severe axial hypotonia, appendicular hypertonia	profound DD	–	+	+
Individual 21	3y (M)[a]	c.2104G>A (p.Ala702Thr) *de novo*	ES (5 m), FM, SE.	hyps, multifocal discharges	normal	severe hypotonia	profound DD: NV, NA	–	+	+
Individual 22	10y (F)	c.2104G>A (p.Ala702Thr) *de novo*	ES (6 m), FM, T, Myo	multifocal discharges	cortical atrophy	profound hypotonia, spastic quadriplegia	profound DD: NV, NA	dyskinesia	+	–
Individual 23	1y (F)[a]	c.2104G>A (p.Ala702Thr) *de novo*	ES (3 m), FM	hyps	T2 hyperintensity in basal ganglia	diffuse hypotonia	profound DD	–	+	+
Individual 24	2y (F)	c.2104G>A (p.Ala702Thr) *de novo*	ES (4 m), FM, Myo	multifocal discharges	normal	severe axial hypotonia	profound DD: NV, NA	–	+	+
Individual 25	7y (M)	c.2104G>C (p.Ala702Pro) *de novo*	unavailable	unavailable	unavailable	hyptonia, spastic quadriplegia	DD	unknown	unknown	unknown
Individual 26	10 m (M)[a]	c.4264A>T (p.Ile1422Phe)	Myo (1d)	burst-suppression	normal	axial hypotonia	profound DD	–	+	+

(*Continued on next page*)

Table 1. *Continued*

	Age (Sex)	Variant (NM_000721.3)	Seizure Types (Age of Onset of First Seizure)	EEG	MRI	Neurological Features	Development	Movement Disorder	Congenital Contractures	Macrocephaly
Individual 27	6y (F)	c.4274C>A (p.Thr1425Asn) *de novo*	ES (5 m)	multifocal discharges	normal	mild hypotonia	severe DD: single words, walks with assistance	–	–	–
Individual 28	4y (F)	c.4274C>A (p.Thr1425Asn) *de novo*	–	not done	normal	hypotonia	severe DD; single words, ambulant	–	–	–
Individual 29	4y (M)	c.4288G>A (p.Gly1430Arg) *de novo*	–	not done	delayed myelination	profound appendicular hypotonia	severe DD; single words, ambulant	–	–	–
Individual 30	2y (F)[a]	c.5159C>G (p.Ala1720Gly) not maternally inherited	ES (3w), Myo, GTCS, At, SE	multifocal discharges	thin corpus callosum	severe axial hypotonia, appendicular hypertonia	profound DD: NV, NA	–	+	–

Abbreviations: At, atonic seizures; CSWS, continuous spike and wave in slow wave sleep; d, days; DD, developmental delay; ES, epileptic spasms; F, female; FIAS, focal impaired awareness seizures; FM, focal motor seizures; gel, gelastic seizures; GTCS, generalized tonic-clonic seizures; hyps, hypsarrhythmia; ID, intellectual disability; m, months; M, male; Myo, myoclonic seizures; NV, non-verbal; NA, non-ambulatory; SE, status epilepticus; T, tonic seizures; w, weeks; y, years. Further clinical details are provided in Table S1.

[a]Deceased, age at death

Hyperkinetic movement disorders were prominent, including severe dystonia in 12/30 (40%) and other dyskinesias in 6/30 (20%) individuals; movement disorders were constant and profoundly disabling in some individuals. For example, in individual 2, dystonic movements were thought to have begun *in utero* and occurred every 2–3 min by 6 months of age and were not relieved by baclofen or benztropine (Videos S1 and S2).

Macrocephaly without other structural abnormalities on brain magnetic resonance imaging was present in 12/28 (43%) individuals for whom data were available. Common dysmorphic features were not observed. Out of 30 individuals, 7 (23%) had died with a median age of death of 2.7 years (range 11 months to 25 years). Reported causes of death were cardiorespiratory failure and status epilepticus.

Seizure Response to Topiramate

Although seizures were resistant to multiple anti-epileptic drugs (AEDs) in most individuals for whom data were available (20/25; 80%), five individuals (1, 15, 16, 21, 27) reported significant improvement in seizure control with topiramate, the only AED noted to have a substantial effect on seizure control in any participants (Table S1). Two individuals (16 and 27) remain seizure free for 2 and 5 years, respectively. However, in individuals 15 and 21, seizures eventually recurred after seizure-free periods of 4 years and 18 months, respectively; individual 21 died following an episode of status epilepticus. Individual 1 reported a substantial reduction in seizure frequency with topiramate, but it was discontinued due to increased sedation. Topiramate had no effect on seizure control in 10/18 (56%) individuals who were prescribed it; 3/18 (17%) individuals who were prescribed topiramate reported a reduction in seizures but were never seizure free.

Genetic Analysis

Missense Variants

Molecular genetic testing identified 14 missense variants in *CACNA1E* (GenBank: NM_000721.3) in 30 unrelated individuals (Table 1). For the 29/30 individuals for whom DNA samples were available for both parents, *de novo* status of the variants and parentage were confirmed. Three recurrent variants—c.1054G>A (p.Gly352Arg) (n = 9), c.2104G>A (p.Ala702Thr) (n = 6), and c.2101A>G (p.Ile701Val) (n = 3)—accounted for 60% of individuals (18/30). One additional variant, c.4274C>A (p.Thr1425Asn), was identified in two individuals. Prominent clustering of *CACNA1E* variants (11/14; 79%) was noted in the cytoplasmic parts of all four S6 segments (Figure 1), which are presumed to form a crucial part of the activation gate in voltage-activated cation channels.[33,34,36]

Loss-of-Function Variants

In addition to the 30 individuals with missense variants, we identified three further individuals with *CACNA1E* variants that introduce premature termination codons predicted to result in haploinsufficiency, with no other

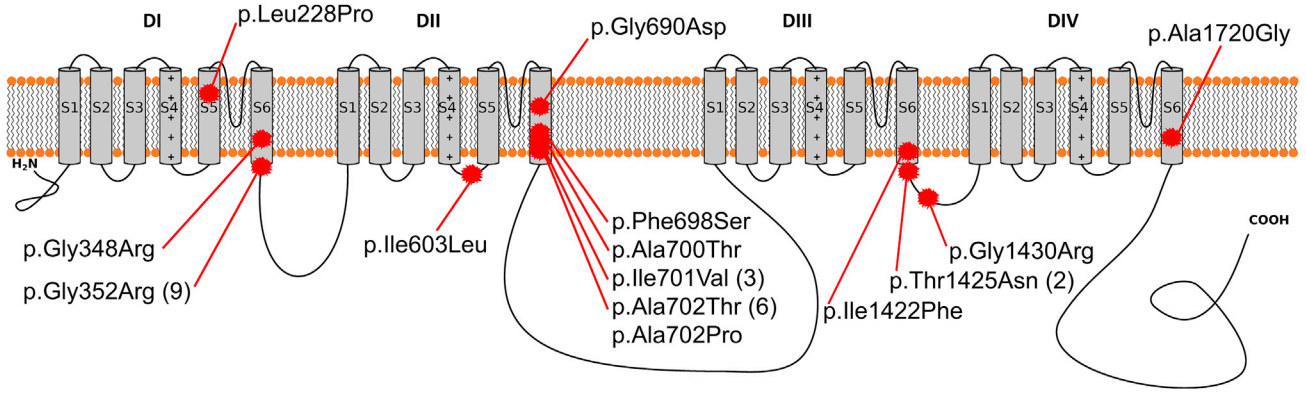

Figure 1. Secondary Structure of the $Ca_v2.3$ Channel with the Distribution of Disease-Causing Missense Variants
Variants are highly clustered in the cytoplasmic ends of all four S6 transmembrane segments, which line the inner pore of the channel and form the activation gate of $Ca_v2.3$ and other voltage-gated cation channels. Numbers in parentheses indicate the number of individuals harboring the variant.

known causative genetic variants identified (individuals 31–33; Table S2). Individual 31 has a mosaic nonsense variant with a mutant allele fraction of 27% (6/22 reads) in peripheral blood leukocytes. In individual 32, a *CACNA1E* frameshift variant was inherited from an apparently unaffected father. Parental DNA samples were unavailable for individual 33, who has a heterozygous germline nonsense variant. All three individuals had comparably milder phenotypes, achieving independent ambulation at 15–18 months and acquiring single words; 2/3 individuals had epilepsy.

Genotype-Phenotype Correlations

Some genotype-phenotype correlations emerged in our cohort of individuals with *CACNA1E*-encephalopathy. Dystonia was a prominent feature in all nine individuals with the recurrent c.1054G>A (p.Gly352Arg) variant. This variant is in close proximity to the c.1042G>C (p.Gly348Arg) variant in individual 2 who also demonstrated profound dystonia. Dystonia was less common in individuals with other variants, only observed in 2/19 (11%) remaining probands, suggesting that variants in the domain I GX_3G motif may predispose to prominent hyperkinetic movement disorders. Two individuals harboring the c.4274C>A (p.Thr1425Asn) variant and one individual with the c.4288G>A (p.Gly1430Arg) variant presented with a comparatively milder clinical picture. All three probands were the only individuals in the cohort to speak single words and walk independently or with assistance, in contrast to the profound impairment in the remainder of the cohort. Two of these probands had not developed seizures by age 4 years, and the other had been seizure free for 5 years and off AEDs at age 6 years.

The six individuals harboring the recurrent c.2104G>A (p.Ala702Thr) variant had a relatively homogeneous phenotype that was representative of the overall *CACNA1E*-encephalopathy phenotype. All individuals had refractory infantile-onset epilepsy, epileptic spasms, severe hypotonia, and profound developmental impairment. Five out of six individuals (83%) harboring the c.2104G>A (p.Ala702Thr) variant had congenital joint contractures and macrocephaly; hypsarrhythmia on EEG consistent with a diagnosis of West syndrome was observed in four of these individuals (67%). Two of these six individuals died in early childhood at ages 1 and 3 years.

Functional Analysis

Domain II S6 Variants

We evaluated the functional effects of three missense variants (p.Phe698Ser, p.Ile701Val, and p.Ala702Thr) located in the cytoplasmic end of the S6 segment of domain II (IIS6; Figure 1). For the IIS6 variants, we performed electrophysiological recordings of tsA201 cells that were transiently transfected with either wild-type or mutant α_{1E}-subunits together with the β_{2d}-subunit, confirmed by the green fluorescence of EGFP which was co-expressed via an internal ribosome entry site (IRES). All three IIS6 variants exhibited consistent abnormalities of activation and inactivation kinetics compared to wild-type channels (Figure 2; Table 2). The activation curve was shifted by approximately −10 mV for all three variants (Figure 2), while the time course of activation was not altered. Additionally, the time course of fast inactivation was significantly slowed, as indicated by an increased residual current after a 400-ms depolarizing pulse normalized to the peak current (r400) (Figures 2 and S1; Table 2).

Domain II S4-S5 Linker Variant

The p.Ile603Leu variant, located in the domain II S4-S5 linker (IIS4-S5; Figure 1), was co-expressed with β_{1b} and $\alpha_2\delta_1$ subunits in tsA201 cells and compared functionally to the wild-type channel. This variant resulted in a massive increase in whole-cell current density (Figures 3 and S2) to a level that in many cases precluded functional biophysical characterization. In a subset of cells where the current could be properly clamped, our analysis revealed a >10 mV hyperpolarizing shift in half activation voltage (Figures 3

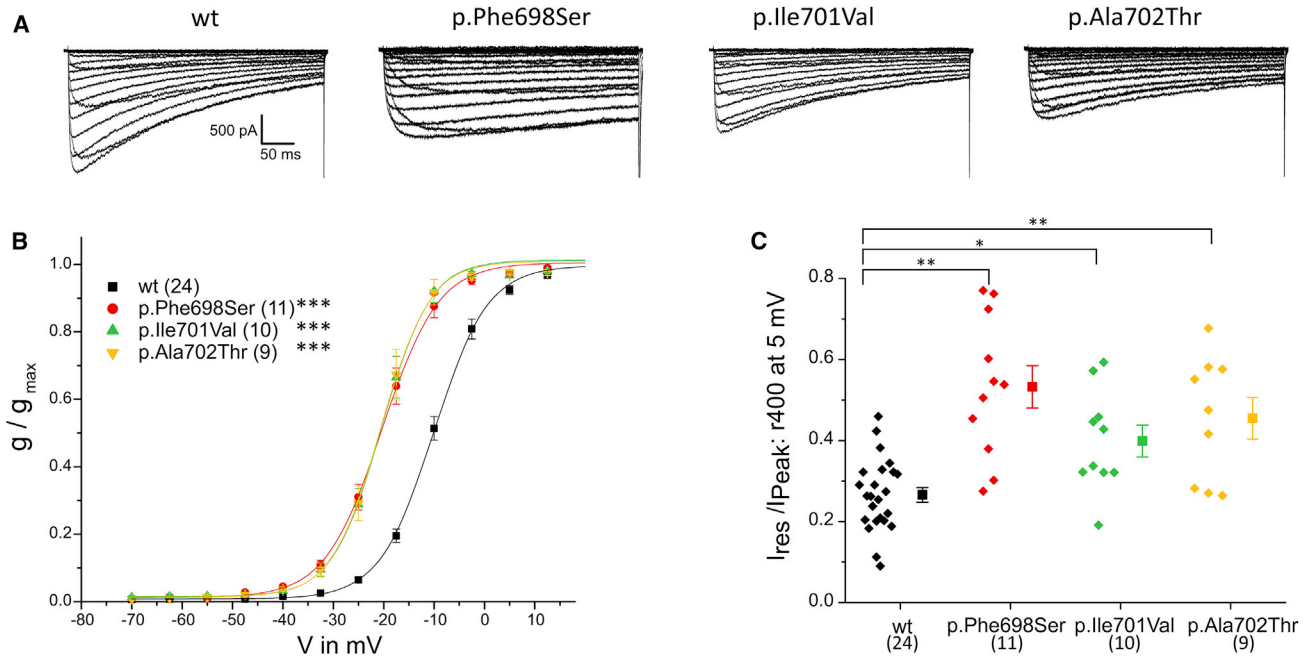

Figure 2. Functional Effects of *CACNA1E* (GenBank: NM_001205293.1) Domain II S6 Variants Introduced into $\alpha_{1E\text{-}1}$ and Co-expressed with β_{2d} in tsA-201 Cells using 15 mM Ba^{2+} as Charge Carrier

(A) Current traces elicited by depolarizing voltage pulses in 7.5-mV steps from a holding potential of −90 mV.

(B) The voltage dependence of activation was similarly and highly significantly shifted for all three variants.

(C) The residual current (r400) at +5 mV was determined by dividing the mean current of the last 10 ms of a 400-ms test pulse (I_{res}) by the peak current (I_{Peak}) of the same pulse.

Numbers in parentheses denote the number of experimental readings per variant. Data are represented as means ± SEM (and in addition all measured values in C). *$p < 0.05$; **$p < 0.01$; ***$p < 0.001$.

and S2; Table 2). There was no significant effect on channel inactivation.

Discussion

Here we describe *CACNA1E*-encephalopathy as a disorder of neuronal calcium channel dysfunction in 30 individuals with disease-causing missense *CACNA1E* variants. All identified individuals with *CACNA1E*-encephalopathy present with similar clinical features, including profound developmental impairment, infantile-onset refractory epilepsy, and severe axial hypotonia. Developmental and epileptic encephalopathies are genetically heterogeneous and can be caused by pathogenic variants in genes encoding other voltage-gated neuronal ion channels, including *SCN2A*, *SCN8A*, *KCNQ2*, and *CACNA1A*.[3,37–39] Some aspects of *CACNA1E*-encephalopathy are clinically similar to other genetic DEEs, including early-onset refractory seizures, developmental impairment, and abnormalities in tone. However, notable features of *CACNA1E*-encephalopathy include prominent hyperkinetic movement disorders, congenital joint contractures, macrocephaly, and early death in a subset of affected individuals.

Functional analysis of several missense variants revealed highly consistent gain-of-function effects, characterized by facilitated voltage-dependent activation, slowed inactivation, and increased current density. Voltage-dependent calcium channel α_1-subunits are responsible for the electrophysiological properties of the channel and are comprised of four homologous domains (I to IV), with each domain containing six transmembrane segments (S1 to S6). The four S6 transmembrane helices line the channel pore,[36] and the structure at the cytoplasmic end of S6 segments contains the presumed activation gate and is crucial in channel gating.[33,34] Disease-causing missense variants in our cohort clustered in cytoplasmic parts of all four S6 transmembrane segments, suggesting that the observed gain-of-function effects perturb the gating properties of the $Ca_V2.3$ channel.

Prior to our discovery of pathogenic variants in *CACNA1E* as a cause of human disease, selected variants had already been artificially introduced into different S6 segments in biophysical and electrophysiological studies to characterize the structure and function of $Ca_V2.3$ channels, and our functional analysis revealed results consistent with previous studies (Figure S3).[33,34] We now identify three previously studied variants in $Ca_V2.3$ (p.Gly352Arg, p.Ile701Val, p.Ala1720Gly) as disease causing in our cohort. Most of the previously investigated variants (including p.Gly352Arg, p.Ile701Val/Gly, and p.Ala1720Gly) also shifted the voltage dependence of activation toward more negative potentials and slowed

Table 2. Main Electrophysiological Parameters of IIS6 and IIS4-S5 Variants Causing Gain-of-Function

	Current Density	Steady-State Activation		Inactivation
	(pA/pF)	$V_{1/2}$ (mV)	k_V (mV)	r400 at +5 mV
IIS6 Variants in $\alpha_{1E\text{-}1} + \beta_{2a}$; 15 mM Ba^{2+}				
Wild-type	−183.1 ± 17.7 (24)	−9.7 ± 0.8 (24)	5.0 ± 1.1 (24)	0.27 ± 0.09 (24)
p.Phe698Ser	−121.4 ± 17.1 (11)	−20.1 ± 1.2 (11)***	5.1 ± 0.7 (11)	0.53 ± 0.05 (11)**
p.Ile701Val	−186.9 ± 27.8 (10)	−20.5 ± 1.2 (10)***	4.3 ± 0.7 (10)	0.40 ± 0.04 (10)*
p.Ala702Thr	−184.5 ± 34.2 (9)	−20.4 ± 1.4 (9)***	4.2 ± 0.3 (9)	0.45 ± 0.05 (9)**
IIS4-S5 Linker Variant $\alpha_{1E\text{-}3} + \beta_{1b} + \alpha_2\delta$; 2 mM Ca^{2+}				τ_{inact} (ms) at +5 mV
Wild-type	−47.8 ± 10.9 (13)	−18.0 ± 1.6 (13)	4.4 ± 0.5 (13)	66.1 ± 8.9 (9)
p.Ile603Leu	−192.3 ± 20.4 (16)****	−29.4 ± 2.7 (10)**	3.1 ± 0.3 (10)	80.6 ± 8.7 (10)
IIS4-S5 Linker Variant $\alpha_{1E\text{-}3} + \beta_{1b} + \alpha_2\delta$; 5 mM Ba^{2+}				τ_{inact} (ms) at +5 mV
Wild-type	−105.9 ± 18.3 (13)	−18.8 ± 1.5 (10)	4.7 ± 0.2 (10)	58.6 ± 3.6 (7)
p.Ile603Leu	−197.5 ± 35.2 (13)*	−31.9 ± 2.1 (10)****	3.7 ± 0.6 (10)	109.9 ± 13.9 (8)**

$V_{1/2}$ is the voltage of half-maximal activation, k_V is a slope factor, r400 is the residual current in a 400-ms lasting pulse to 5 mV normalized to the peak current of the same trace, τ_{inact} is the exponential time constant of inactivation; numbers in brackets indicate the number of cells that were analyzed for this parameter, data are represented as mean ± SEM; *p < 0.05; **p < 0.01; ***p < 0.001; ****p < 0.0001.

the inactivation time course.[33,34] The p.Gly348Arg and the recurrent p.Gly352Arg variants are part of a highly conserved GX_3G motif that is located in the cytoplasmic end of the domain I S6 segment and plays an essential role in voltage-dependent inactivation of voltage-gated calcium channels. Notably, Gly348 and Gly352 in $Ca_v2.3$ are paralogous to Gly402 and Gly406 in $Ca_v1.2$ encoded by *CACNA1C* which are altered (p.Gly402Ser, p.Gly406Arg) in Timothy syndrome, a severe developmental disorder with fatal cardiac arrhythmia and autism.[6,7]

Although most disease-causing variants cluster in S6 transmembrane segments, the identified p.Ile603Leu variant is located in the linker between segments S4 and S5 in domain II. Functional analysis also identified strong gain-of-function properties for this variant, revealing increased current density and facilitated activation. These observed gain-of-function effects are also consistent with prior $Ca_V2.3$ biophysical studies showing that the domain II S4-S5 linker region is important for regulating channel activation.[40]

In contrast to *de novo* missense variants with a gain-of-function effect, the role of *CACNA1E* haploinsufficiency is less clear. We identify three individuals with loss-of-function *CACNA1E* variants with comparably milder phenotypes. In one case the frameshift variant was transmitted from an unaffected parent. Several loss-of-function variants are reported in the gnomAD database, but loss-of-function variants do not appear to be well tolerated in healthy individuals (pLI = 1.0).[32]

The AEDs topiramate and lamotrigine target $Ca_V2.3$ channels and reduce R-type calcium currents.[41,42] Five individuals with *CACNA1E*-encephalopathy achieved seizure freedom on topiramate therapy, which was the only AED to meaningfully impact seizure control among any affected individuals. These data indicate that topiramate, an R-type channel blocker, has a positive effect in some individuals, possibly because its inhibitory mechanism targets the gain-of-function pathophysiology we have demonstrated *in vitro*. This is in stark contrast to a large number of other AEDs that did not show a sustained beneficial effect in more than a single individual.

In summary, we identified a genetic DEE associated with *de novo* missense variants in *CACNA1E* in 30 individuals, with notable features of congenital contractures and macrocephaly in many individuals. Profound impairment with hypotonia and movement disorders were often part of the *CACNA1E*-encephalopathy phenotype. Functional analysis revealed dramatic gain-of-function effects, indicating increased calcium inward currents that may affect neuronal excitability and synaptic transmission. The identification of pathogenic gain-of-function variants in *CACNA1E* in these individuals adds to the growing list of channelopathies causing neurodevelopmental disorders and DEEs. We implicate facilitated R-type calcium currents as a disease mechanism in human epilepsy, which provides a promising target for the development of precision medicines for this devastating disease.

Accession Numbers

The accession number for the $Ca_V2.3$ $\alpha_{1E\text{-}3}$ construct used in this paper is GenBank: L29385.1

Supplemental Data

Supplemental Data include Supplemental Methods, three figures, two tables, and two videos and can be found with this article online at https://doi.org/10.1016/j.ajhg.2018.09.006.

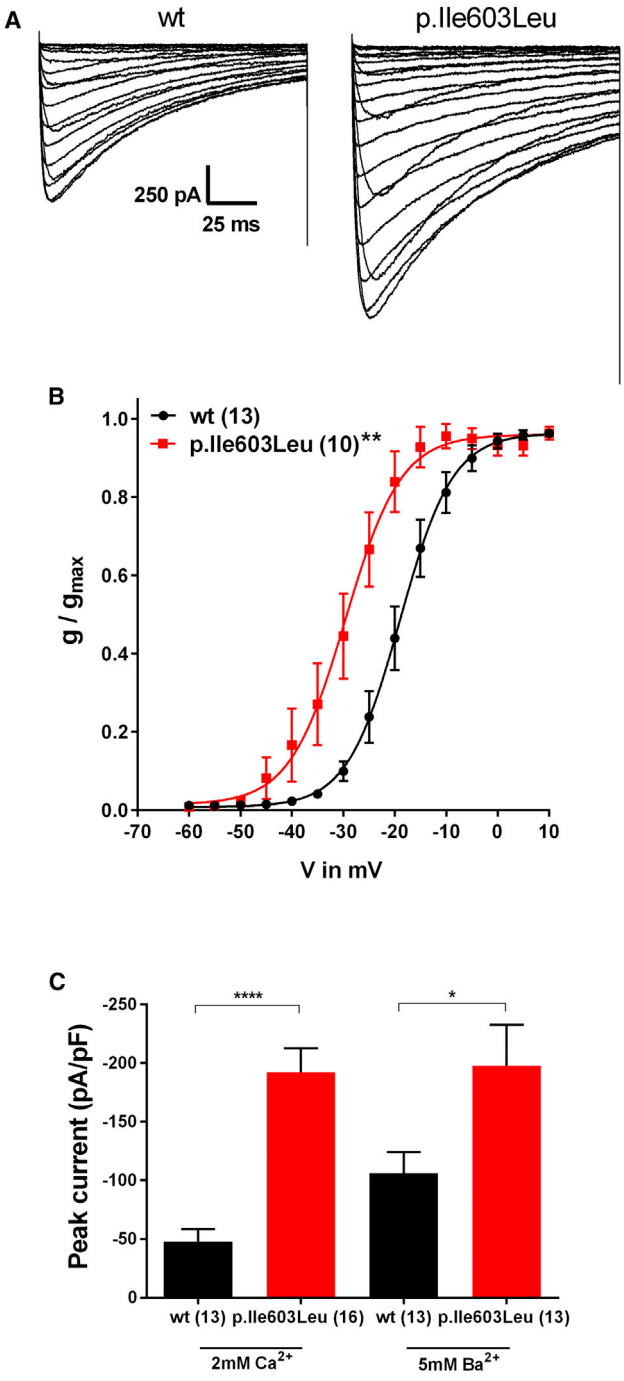

Figure 3. Functional Effects of the *CACNA1E* (GenBank: NM_001205293.1) Domain II S4-S5 Variant p.Ile603Leu Introduced into $\alpha_{1E\text{-}3}$ and Co-expressed with β_{1b} and $\alpha_2\delta_1$ in tsA-201 Cells

(A) Current traces elicited by depolarizing voltage pulses in 5 mV steps from a holding potential of −100 mV as recorded with 2 mM Ca^{2+} as charge carrier.

(B) Voltage dependence of activation recorded in 2 mM Ca^{2+} revealing a significant difference between WT and mutant channels. Numbers in parentheses denote the number of experimental readings per variant.

(C) Mean peak current densities for WT and p.Ile603Leu channels recorded in 2 mM Ca^{2+} or 5 mM Ba^{2+}.

Data are represented as mean ± SEM. Numbers in parentheses denote the number of experimental readings per variant. Asterisks denote statistical significance (Student's t test, *$p \leq 0.05$, **$p \leq 0.01$, and ****$p \leq 0.0001$).

Acknowledgments

We thank the participants and families for participating in our study. R.J.L. is supported by a Siegmund-Kiener stipend for medical doctoral students at the Hertie Institute of Clinical Brain Research. C.T.M. is supported by the Lennox-Gastaut Syndrome Foundation (LGSF). M.A.G. holds fellowships from Alberta Innovates and CIHR. M.A. Corbett is supported by The Channel 7 Children's Research Foundation and the Cerebral Palsy Alliance Research Foundation. R.W. is supported by The Brian and Caris Chan Family Foundation. J.C.J. is supported by a Rutherford Discovery Fellowship from the New Zealand Government, administered by the Royal Society of New Zealand. Bioinformatic analysis was supported by the New Zealand eScience Infrastructure. L.G.S. is supported by the Health Research Council of New Zealand and Cure Kids New Zealand. G.W.Z. is supported by the Canadian Institutes of Health Research (CIHR) and is a Canada Research Chair. A.S.-J., K.J.C., and F.L.R. were supported by Cambridge BRC and the National Institute for Health Research England (NIHR) for the NIHR BioResource (grant RG65966). I.E.S. is supported by the National Health and Medical Research Council of Australia, National Institutes of Health, Australian Research Council, Health Research Council of New Zealand, CURE, and March of Dimes. I. Helbig, U.B.S.H., and H.L. are supported by the DFG Research Unit FOR 2715 (grants He5415/7-1, He8155/1-1, Le1030/16-1). H.C.M. is supported by the NIH (NINDS NS069605). We are thankful to the Deciphering Developmental Disorders (DDD) study. The DDD study (Cambridge South REC approval 10/H0305/83 and the Republic of Ireland REC GEN/284/12) presents independent research commissioned by the Health Innovation Challenge Fund (grant number HICF-1009-003), a parallel funding partnership between the Wellcome Trust and the Department of Health, and the Wellcome Trust Sanger Institute (grant number WT098051). The views expressed in this publication are those of the authors and not necessarily those of the Wellcome Trust or the Department of Health.

Declaration of Interests

I.E.S. has received support from and/or has served as a paid consultant for UCB, Eisai, Athena Diagnostics, GlaxoSmithKline, Biocodex, Biomarin, and Nutricia and may accrue future revenue on pending patent WO61/010176 (filed: 2008): Therapeutic Compound. H.C.M. is a member of scientific advisory boards for Lennox Gastaut Syndrome Foundation, Dravet Syndrome Foundation, and SPARK. The remaining authors declare no competing interests.

Received: July 20, 2018
Accepted: September 17, 2018
Published: October 18, 2018

Web Resources

GenBank, https://www.ncbi.nlm.nih.gov/genbank/
GeneMatcher, https://genematcher.org/
gnomAD Browser, http://gnomad.broadinstitute.org/
OMIM, http://www.omim.org/

References

1. McTague, A., Howell, K.B., Cross, J.H., Kurian, M.A., and Scheffer, I.E. (2016). The genetic landscape of the epileptic

encephalopathies of infancy and childhood. Lancet Neurol. *15*, 304–316.
2. EuroEPINOMICS-RES Consortium; Epilepsy Phenome/Genome Project; and Epi4K Consortium (2014). De novo mutations in synaptic transmission genes including DNM1 cause epileptic encephalopathies. Am. J. Hum. Genet. *95*, 360–370.
3. Epi4K Consortium (2016). De novo mutations in SLC1A2 and CACNA1A are important causes of epileptic encephalopathies. Am. J. Hum. Genet. *99*, 287–298.
4. Rajakulendran, S., Kaski, D., and Hanna, M.G. (2012). Neuronal P/Q-type calcium channel dysfunction in inherited disorders of the CNS. Nat. Rev. Neurol. *8*, 86–96.
5. Imbrici, P., Jaffe, S.L., Eunson, L.H., Davies, N.P., Herd, C., Robertson, R., Kullmann, D.M., and Hanna, M.G. (2004). Dysfunction of the brain calcium channel CaV2.1 in absence epilepsy and episodic ataxia. Brain *127*, 2682–2692.
6. Splawski, I., Timothy, K.W., Decher, N., Kumar, P., Sachse, F.B., Beggs, A.H., Sanguinetti, M.C., and Keating, M.T. (2005). Severe arrhythmia disorder caused by cardiac L-type calcium channel mutations. Proc. Natl. Acad. Sci. USA *102*, 8089–8096, discussion 8086–8088.
7. Splawski, I., Timothy, K.W., Sharpe, L.M., Decher, N., Kumar, P., Bloise, R., Napolitano, C., Schwartz, P.J., Joseph, R.M., Condouris, K., et al. (2004). Ca(V)1.2 calcium channel dysfunction causes a multisystem disorder including arrhythmia and autism. Cell *119*, 19–31.
8. Scholl, U.I., Goh, G., Stölting, G., de Oliveira, R.C., Choi, M., Overton, J.D., Fonseca, A.L., Korah, R., Starker, L.F., Kunstman, J.W., et al. (2013). Somatic and germline CACNA1D calcium channel mutations in aldosterone-producing adenomas and primary aldosteronism. Nat. Genet. *45*, 1050–1054.
9. Pinggera, A., Mackenroth, L., Rump, A., Schallner, J., Beleggia, F., Wollnik, B., and Striessnig, J. (2017). New gain-of-function mutation shows CACNA1D as recurrently mutated gene in autism spectrum disorders and epilepsy. Hum. Mol. Genet. *26*, 2923–2932.
10. Coutelier, M., Blesneac, I., Monteil, A., Monin, M.L., Ando, K., Mundwiller, E., Brusco, A., Le Ber, I., Anheim, M., Castrioto, A., et al. (2015). A recurrent mutation in CACNA1G alters Cav3.1 T-Type calcium-channel conduction and causes autosomal-dominant cerebellar ataxia. Am. J. Hum. Genet. *97*, 726–737.
11. Morino, H., Matsuda, Y., Muguruma, K., Miyamoto, R., Ohsawa, R., Ohtake, T., Otobe, R., Watanabe, M., Maruyama, H., Hashimoto, K., and Kawakami, H. (2015). A mutation in the low voltage-gated calcium channel CACNA1G alters the physiological properties of the channel, causing spinocerebellar ataxia. Mol. Brain *8*, 89.
12. Chemin, J., Siquier-Pernet, K., Nicouleau, M., Barcia, G., Ahmad, A., Medina-Cano, D., Hanein, S., Altin, N., Hubert, L., Bole-Feysot, C., et al. (2018). De novo mutation screening in childhood-onset cerebellar atrophy identifies gain-of-function mutations in the CACNA1G calcium channel gene. Brain *141*, 1998–2013.
13. Williams, M.E., Marubio, L.M., Deal, C.R., Hans, M., Brust, P.F., Philipson, L.H., Miller, R.J., Johnson, E.C., Harpold, M.M., and Ellis, S.B. (1994). Structure and functional characterization of neuronal alpha 1E calcium channel subtypes. J. Biol. Chem. *269*, 22347–22357.
14. Wormuth, C., Lundt, A., Henseler, C., Müller, R., Broich, K., Papazoglou, A., and Weiergräber, M. (2016). Review: $Ca_v2.3$ R-type voltage-gated Ca^{2+} channels - functional implications in convulsive and non-convulsive seizure activity. Open Neurol. J. *10*, 99–126.
15. Parajuli, L.K., Nakajima, C., Kulik, A., Matsui, K., Schneider, T., Shigemoto, R., and Fukazawa, Y. (2012). Quantitative regional and ultrastructural localization of the Ca(v)2.3 subunit of R-type calcium channel in mouse brain. J. Neurosci. *32*, 13555–13567.
16. Weiergräber, M., Henry, M., Krieger, A., Kamp, M., Radhakrishnan, K., Hescheler, J., and Schneider, T. (2006). Altered seizure susceptibility in mice lacking the Ca(v)2.3 E-type Ca2+ channel. Epilepsia *47*, 839–850.
17. Weiergräber, M., Henry, M., Radhakrishnan, K., Hescheler, J., and Schneider, T. (2007). Hippocampal seizure resistance and reduced neuronal excitotoxicity in mice lacking the Cav2.3 E/R-type voltage-gated calcium channel. J. Neurophysiol. *97*, 3660–3669.
18. Heyne, H.O., Singh, T., Stamberger, H., Abou Jamra, R., Caglayan, H., Craiu, D., De Jonghe, P., Guerrini, R., Helbig, K.L., Koeleman, B.P.C., et al.; EuroEPINOMICS RES Consortium (2018). De novo variants in neurodevelopmental disorders with epilepsy. Nat. Genet. *50*, 1048–1053.
19. Sobreira, N., Schiettecatte, F., Valle, D., and Hamosh, A. (2015). GeneMatcher: a matching tool for connecting investigators with an interest in the same gene. Hum. Mutat. *36*, 928–930.
20. Allen, A.S., Berkovic, S.F., Cossette, P., Delanty, N., Dlugos, D., Eichler, E.E., Epstein, M.P., Glauser, T., Goldstein, D.B., Han, Y., et al.; Epi4K Consortium; and Epilepsy Phenome/Genome Project (2013). De novo mutations in epileptic encephalopathies. Nature *501*, 217–221.
21. Deciphering Developmental Disorders Study (2017). Prevalence and architecture of de novo mutations in developmental disorders. Nature *542*, 433–438.
22. Carss, K.J., Arno, G., Erwood, M., Stephens, J., Sanchis-Juan, A., Hull, S., Megy, K., Grozeva, D., Dewhurst, E., Malka, S., et al.; NIHR-BioResource Rare Diseases Consortium (2017). Comprehensive rare variant analysis via whole-genome sequencing to determine the molecular pathology of inherited retinal disease. Am. J. Hum. Genet. *100*, 75–90.
23. de Goede, C., Yue, W.W., Yan, G., Ariyaratnam, S., Chandler, K.E., Downes, L., Khan, N., Mohan, M., Lowe, M., and Banka, S. (2016). Role of reverse phenotyping in interpretation of next generation sequencing data and a review of INPP5E related disorders. Eur. J. Paediatr. Neurol. *20*, 286–295.
24. Scheffer, I.E., Berkovic, S., Capovilla, G., Connolly, M.B., French, J., Guilhoto, L., Hirsch, E., Jain, S., Mathern, G.W., Moshé, S.L., et al. (2017). ILAE classification of the epilepsies: Position paper of the ILAE Commission for Classification and Terminology. Epilepsia *58*, 512–521.
25. Fisher, R.S., Cross, J.H., French, J.A., Higurashi, N., Hirsch, E., Jansen, F.E., Lagae, L., Moshé, S.L., Peltola, J., Roulet Perez, E., et al. (2017). Operational classification of seizure types by the International League Against Epilepsy: Position Paper of the ILAE Commission for Classification and Terminology. Epilepsia *58*, 522–530.
26. Retterer, K., Juusola, J., Cho, M.T., Vitazka, P., Millan, F., Gibellini, F., Vertino-Bell, A., Smaoui, N., Neidich, J., Monaghan, K.G., et al. (2016). Clinical application of whole-exome sequencing across clinical indications. Genet. Med. *18*, 696–704.
27. Farwell, K.D., Shahmirzadi, L., El-Khechen, D., Powis, Z., Chao, E.C., Tippin Davis, B., Baxter, R.M., Zeng, W.,

Mroske, C., Parra, M.C., et al. (2015). Enhanced utility of family-centered diagnostic exome sequencing with inheritance model-based analysis: results from 500 unselected families with undiagnosed genetic conditions. Genet. Med. *17*, 578–586.

28. Faundes, V., Newman, W.G., Bernardini, L., Canham, N., Clayton-Smith, J., Dallapiccola, B., Davies, S.J., Demos, M.K., Goldman, A., Gill, H., et al.; Clinical Assessment of the Utility of Sequencing and Evaluation as a Service (CAUSES) Study; and Deciphering Developmental Disorders (DDD) Study (2018). Histone lysine methylases and demethylases in the landscape of human developmental disorders. Am. J. Hum. Genet. *102*, 175–187.
29. Lindy, A.S., Bupp, C.P., McGee, S.J., Steed, E., Stevenson, R.E., Basehore, M.J., and Friez, M.J. (2014). Truncating mutations in LRP4 lead to a prenatal lethal form of Cenani-Lenz syndrome. Am. J. Med. Genet. A. *164A*, 2391–2397.
30. Myers, C.T., Hollingsworth, G., Muir, A.M., Schneider, A.L., Thuesmunn, Z., Knupp, A., King, C., Lacroix, A., Mehaffey, M.G., Berkovic, S.F., et al. (2018). Parental mosaicism in "de novo" epileptic encephalopathies. N. Engl. J. Med. *378*, 1646–1648.
31. Richards, S., Aziz, N., Bale, S., Bick, D., Das, S., Gastier-Foster, J., Grody, W.W., Hegde, M., Lyon, E., Spector, E., et al.; ACMG Laboratory Quality Assurance Committee (2015). Standards and guidelines for the interpretation of sequence variants: a joint consensus recommendation of the American College of Medical Genetics and Genomics and the Association for Molecular Pathology. Genet. Med. *17*, 405–424.
32. Lek, M., Karczewski, K.J., Minikel, E.V., Samocha, K.E., Banks, E., Fennell, T., O'Donnell-Luria, A.H., Ware, J.S., Hill, A.J., Cummings, B.B., et al.; Exome Aggregation Consortium (2016). Analysis of protein-coding genetic variation in 60,706 humans. Nature *536*, 285–291.
33. Raybaud, A., Baspinar, E.E., Dionne, F., Dodier, Y., Sauvé, R., and Parent, L. (2007). The role of distal S6 hydrophobic residues in the voltage-dependent gating of CaV2.3 channels. J. Biol. Chem. *282*, 27944–27952.
34. Raybaud, A., Dodier, Y., Bissonnette, P., Simoes, M., Bichet, D.G., Sauvé, R., and Parent, L. (2006). The role of the GX9GX3G motif in the gating of high voltage-activated Ca2+ channels. J. Biol. Chem. *281*, 39424–39436.
35. Vajna, R., Klöckner, U., Pereverzev, A., Weiergräber, M., Chen, X., Miljanich, G., Klugbauer, N., Hescheler, J., Perez-Reyes, E., and Schneider, T. (2001). Functional coupling between 'R-type' Ca2+ channels and insulin secretion in the insulinoma cell line INS-1. Eur. J. Biochem. *268*, 1066–1075.
36. Jiang, Y., Lee, A., Chen, J., Cadene, M., Chait, B.T., and MacKinnon, R. (2002). Crystal structure and mechanism of a calcium-gated potassium channel. Nature *417*, 515–522.
37. Wolff, M., Johannesen, K.M., Hedrich, U.B.S., Masnada, S., Rubboli, G., Gardella, E., Lesca, G., Ville, D., Milh, M., Villard, L., et al. (2017). Genetic and phenotypic heterogeneity suggest therapeutic implications in SCN2A-related disorders. Brain *140*, 1316–1336.
38. Gardella, E., Marini, C., Trivisano, M., Fitzgerald, M.P., Alber, M., Howell, K.B., Darra, F., Siliquini, S., Bölsterli, B.K., Masnada, S., et al. (2018). The phenotype of *SCN8A* developmental and epileptic encephalopathy. Neurology *91*, e1112–e1124.
39. Millichap, J.J., Park, K.L., Tsuchida, T., Ben-Zeev, B., Carmant, L., Flamini, R., Joshi, N., Levisohn, P.M., Marsh, E., Nangia, S., et al. (2016). KCNQ2 encephalopathy: Features, mutational hot spots, and ezogabine treatment of 11 patients. Neurol Genet *2*, e96.
40. Wall-Lacelle, S., Hossain, M.I., Sauvé, R., Blunck, R., and Parent, L. (2011). Double mutant cycle analysis identified a critical leucine residue in the IIS4S5 linker for the activation of the Ca(V)2.3 calcium channel. J. Biol. Chem. *286*, 27197–27205.
41. Kuzmiski, J.B., Barr, W., Zamponi, G.W., and MacVicar, B.A. (2005). Topiramate inhibits the initiation of plateau potentials in CA1 neurons by depressing R-type calcium channels. Epilepsia *46*, 481–489.
42. Hainsworth, A.H., McNaughton, N.C., Pereverzev, A., Schneider, T., and Randall, A.D. (2003). Actions of sipatrigine, 202W92 and lamotrigine on R-type and T-type Ca2+ channel currents. Eur. J. Pharmacol. *467*, 77–80.